The Astrophysical Journal Supplement Series, 229:31 (7pp), 2017 April doi:10.3847/1538-4365/229/2/31

The InterPlanetary Network Supplement to the Second *Fermi* GBM Catalog of Cosmic Gamma-Ray Bursts

K. Hurley[1], R. L. Aptekar[2], S. V. Golenetskii[2], D. D. Frederiks[2], D. S. Svinkin[2], V. D. Pal'shin[3], M. S. Briggs[4], C. Meegan[4], V. Connaughton[5], J. Goldsten[6], W. Boynton[7], C. Fellows[7], K. Harshman[7], I. G. Mitrofanov[8], D. V. Golovin[8], A. S. Kozyrev[8], M. L. Litvak[8], A. B. Sanin[8], A. Rau[9], A. von Kienlin[9], X. Zhang[9], K. Yamaoka[10,19], Y. Fukazawa[11], M. Ohno[11], M. Tashiro[12], Y. Terada[12], S. Barthelmy[13], T. Cline[13,20], N. Gehrels[13], J. Cummings[14,21], H. A. Krimm[15,21], D. M. Smith[16], E. Del Monte[17], M. Feroci[17], and M. Marisaldi[18]

[1] University of California, Berkeley, Space Sciences Laboratory, 7 Gauss Way, Berkeley, CA 94720-7450, USA; khurley@ssl.berkeley.edu
[2] Ioffe Institute, Politekhnicheskaya 26, St. Petersburg 194021, Russia
[3] Vedeneeva 2-31, St. Petersburg, Russia
[4] University of Alabama in Huntsville, NSSTC, 320 Sparkman Drive, Huntsville, AL 35805, USA
[5] Universities Space Research Association, NSSTC, 320 Sparkman Drive, Huntsville, AL 35805, USA
[6] Applied Physics Laboratory, Johns Hopkins University, Laurel, MD 20723, USA
[7] University of Arizona, Department of Planetary Sciences, Tucson, Arizona 85721, USA
[8] Space Research Institute, 84/32, Profsoyuznaya, Moscow 117997, Russia
[9] Max-Planck-Institut für extraterrestrische Physik, Giessenbachstrasse, Postfach 1312, Garching, D-85748, Germany
[10] Division of Particle and Astrophysical Science, Graduate School of Science, Nagoya University, Furo-cho, Chikusa-ku, Nagoya 464-8602, Japan
[11] Department of Physics, Hiroshima University, 1-3-1 Kagamiyama, Higashi-Hiroshima, Hiroshima 739-8526, Japan
[12] Department of Physics, Saitama University, 255 Shimo-Okubo, Sakura-ku, Saitama-shi, Saitama 338-8570, Japan
[13] NASA Goddard Space Flight Center, Code 661, Greenbelt, MD 20771, USA
[14] UMBC/CRESST/NASA Goddard Space Flight Center, Code 661, Greenbelt, MD 20771, USA
[15] CRESST/NASA Goddard Space Flight Center, Code 661, Greenbelt, MD 20771, USA
[16] Physics Department and Santa Cruz Institute for Particle Physics, University of California, Santa Cruz, Santa Cruz, CA 95064, USA
[17] INAF/IAPS, via Fosso del Cavaliere 100, I-00133, Roma, Italy
[18] Birkeland Center for Space Science, Department of Physics and Technology, University of Bergen, Norway
Received 2016 September 27; revised 2016 November 23; accepted 2016 November 30; published 2017 March 29

Abstract

InterPlanetary Network (IPN) data are presented for the gamma-ray bursts in the second *Fermi* Gamma-Ray Burst Monitor (GBM) catalog. Of the 462 bursts in that catalog between 2010 July 12 and 2012 July 11, 428, or 93%, were observed by at least 1 other instrument in the 9-spacecraft IPN. Of the 428, the localizations of 165 could be improved by triangulation. For these bursts, triangulation gives one or more annuli whose half-widths vary between about 2.′3° and 16°, depending on the peak flux, fluence, time history, arrival direction, and the distance between the spacecraft. We compare the IPN localizations with the GBM 1σ, 2σ, and 3σ error contours and find good agreement between them. The IPN 3σ error boxes have areas between about 8 square arcminutes and 380 square degrees, and are an average of 2500 times smaller than the corresponding GBM 3σ localizations. We identify four bursts in the IPN/GBM sample whose origins were given as "uncertain," but may in fact be cosmic. This leads to an estimate of over 99% completeness for the GBM catalog.

Key words: catalogs – gamma-ray burst: general

Supporting material: figure set, machine-readable tables

1. Introduction

This is the 13th catalog of gamma-ray burst (GRB) localizations obtained by arrival time analysis, or "triangulation" between the spacecraft in the 3rd InterPlanetary Network (IPN; Table 1). Here we present the localization data for 165 bursts that occurred during the second two-year period (2010 July 12 to 2012 July 11) covered by the second *Fermi* Gamma-Ray Burst Monitor (GBM) GRB catalog (von Kienlin et al. 2014). Since the composition of the IPN for this period was identical to the one during the first *Fermi* catalog (Paciesas et al. 2012; Hurley et al. 2013), we present only a brief discussion of the instrumentation and techniques in Section 2. Section 3 contains the localization data, which are also available on the IPN website.[23] Section 4 presents the statistics of the localizations, and we present our conclusions in Section 5.

2. Technique, Instrumentation, Calibration, and Sensitivity

The triangulation technique utilized for the present catalog is identical to that used for the first IPN/GBM catalog; the details may be found in Hurley et al. (2013). Also, the missions and experiments comprising the IPN are the same. The IPN consisted of *Konus-Wind*, at up to approximately 5 light-seconds from Earth (Aptekar et al. 1995); *Mars Odyssey*, in orbit around Mars at up to 1250 light-seconds from Earth (Hurley et al. 2006); the *International Gamma-Ray Laboratory* (*INTEGRAL*), in an eccentric Earth orbit at up to 0.5 light-seconds from Earth

[19] Institute for Space-Earth Environmental Research (ISEE), Nagoya University, Furo-cho, Chikusa-ku, Nagoya 464-8601, Japan.
[20] Emeritus.
[21] Joint Center for Astrophysics, University of Maryland, Baltimore County, 1000 Hilltop Circle, Baltimore, MD 21250.
[22] Universities Space Research Association, 10211 Wincopin Circle, Suite 500, Columbia, MD 21044.
[23] http://ssl.berkeley.edu/ipn3/index.html

Table 1
Recent IPN Catalogs of Gamma-Ray Bursts

Years Covered	Number of GRBs	Description
1990–1992	16	*Ulysses, Pioneer Venus Orbiter*, WATCH, SIGMA, PHEBUS GRBs[a]
1990–1994	56	*Granat*-WATCH supplement[b]
1991–1992	37	*Pioneer Venus Orbiter, Compton Gamma-Ray Observatory, Ulysses* GRBs[c]
1991–1994	218	BATSE 3B supplement[d]
1991–2000	211	BATSE untriggered burst supplement[e]
1992–1993	9	*Mars Observer* GRBs[f]
1994–1996	147	BATSE 4Br supplement[g]
1994–2010	271	Konus short bursts[h]
1996–2000	343	BATSE 5B supplement[i]
1996–2002	475	*BeppoSAX* supplement[j]
2000–2006	226	HETE-2 supplement[k]
2008–2010	149	First GBM supplement[l]
2010–2012	165	Second GBM supplement[m]

Notes.
[a] Hurley et al. (2000b).
[b] Hurley et al. (2000c).
[c] Laros et al. (1998).
[d] Hurley et al. (1999a).
[e] Hurley et al. (2005).
[f] Laros et al. (1997).
[g] Hurley et al. (1999b).
[h] Pal'shin et al. (2013).
[i] Hurley et al. (2011a).
[j] Hurley et al. (2010).
[k] Hurley et al. (2011b).
[l] Hurley et al. (2013).
[m] Present catalog.

(Rau et al. 2005); *Mercury Surface, Space Environment, Geochemistry, and Ranging* mission (*MESSENGER*), in an eccentric orbit around Mercury beginning 2011 March 18, up to 690 light-seconds from Earth (Gold et al. 2001); and *Ramaty High Energy Solar Spectroscopic Imager* (*RHESSI*) (Smith et al. 2002), *Swift* (Gehrels et al. 2004), *Fermi* (Meegan et al. 2009), *Suzaku* (Takahashi et al. 2007; Yamaoka et al. 2009), and *AGILE* (Del Monte et al. 2008; Marisaldi et al. 2008; Tavani et al. 2009), all in low-Earth orbit. The IPN sensitivity, too, was unchanged: the probabilities of IPN detections of a GRB are increasing functions of peak flux and fluence, and are 50% or greater for peak fluxes in the range 1–3 photons cm^{-2} s^{-1} and for fluences in the range 1–3 $\times$ 10^{-6} erg cm^{-2}. More details, including a discussion of calibration, are given in Hurley et al. (2013).

Each cosmic burst, and some bursts designated "uncertain," detected by the GBM were searched for in the IPN data; GBM localizations were used to calculate arrival time windows for the interplanetary spacecraft, but the total crossing time windows defined by light-travel times were examined in all cases. The detections are given in Table 2. *Konus* and *Suzaku* can detect bursts in both a triggered (2–64 ms time resolution) and an untriggered (1–3 s time resolution) mode, and both modes are counted as detections in this table. Also, detections by several instruments that are not in the IPN have been reported in the table, namely the *Fermi* LAT (Large Area Telescope, Atwood et al. 2009), *Monitor of All-sky X-ray Image* (*MAXI*, Serino et al. 2014), and *Interplanetary Kite-craft Accelerated by Radiation Of the Sun* (*IKAROS*, Yonetoku et al. 2011). The statistics of the number of events detected by each spacecraft are given in Table 3, and the number of bursts detected by *N* spacecraft can be found in Table 4.

Whenever *Konus* (in triggered, high time resolution mode), *Odyssey*, or *MESSENGER* detected the burst, we calculated one or two annuli, depending on whether the event was observed by two or three widely separated experiments. These are given in Table 5, and figures may be found in figure set 1; an example is shown in Figure 1. When three widely separated instruments observe a burst, the result is two annuli that generally intersect to define two small error boxes. The GBM error circle or *Konus'* ecliptic latitude response may be used to distinguish the correct one. A number of degenerate cases can occur in a three-spacecraft triangulation, such as close alignments of Mercury, the Earth, and Mars, resulting in annuli that cross at a grazing intersection; they are discussed in Hurley et al. (2011a). When *Konus*, *Odyssey*, *MESSENGER* and a near-Earth spacecraft (including *INTEGRAL*) detect an event, its position is over-determined, and a goodness-of-fit can be derived, and an error ellipse can be generated (Hurley et al. 2000a). Although these smaller error regions can be derived for many events in this catalog, we do not quote them here because their curvature, like that of the annuli they are derived from, can render a simple parameterization inaccurate.

A novel feature of this catalog is the use of newly available 1σ, 2σ, and 3σ GBM error contours (as opposed to the error circle approximations in the previous IPN/GBM catalog); the techniques for producing them are discussed in Connaughton et al. (2015). These regions include both statistical and systematic uncertainties. Table 6 gives the coordinates of the IPN error regions. If there is one triangulation annulus, these are the four intersections of the annulus with the GBM 3σ error contour (e.g., GRB100722096, Figure 5 in figure set 1); if there are two annuli, they are the four intersections of the two annuli (e.g., GRB100713980, Figure 1). In general, the triangulation annuli are small circles on the celestial sphere, so their curvatures may not be negligible, and thus a simple, four-corner error box cannot always be defined accurately (e.g., GRB100805845, Figure 8 in figure set 1). In two cases (GRB101206036, Figure 1.37 in figure set 1, and GRB110717180, Figure 1.81 in figure set 1), GBM contours were not available, and the 1σ statistical-only error circles are shown. IPN annulus widths are often the same size as, or smaller than, *Fermi* LAT error circle radii, and can therefore reduce the areas of LAT localizations. On the other hand, the IPN localizations in this catalog do not improve *Swift* -BAT or *INTEGRAL*-IBIS error circles, and have therefore not been included here.

3. Tables of IPN Localizations

The 9 columns in Table 5 give: (1) the designation of the burst, in the *Fermi* format, which is GRByymmddfff, for the year, month, day, and fraction of the day, (2) the R.A. of the center of the first IPN annulus, (3) the decl. of the center of the first IPN annulus, (4) the angular radius $R_{\rm IPN1}$ of the first IPN annulus, (5) the half-width δ $R_{\rm IPN1}$ of the first IPN annulus; the 3σ (statistical plus systematic) confidence annulus is given by $R_{\rm IPN1} \pm \delta R_{\rm IPN1}$, (6) the R.A. of the center of the second IPN annulus, (7) the decl. of the center of the second IPN annulus, (8) the angular radius $R_{\rm IPN2}$ of the second IPN annulus, (9) the half-width δ $R_{\rm IPN2}$ of the second IPN annulus; the 3σ (statistical plus systematic) confidence annulus is given by $R_{\rm IPN2} \pm \delta R_{\rm IPN2}$. All

Table 2
428 IPN/GBM Gamma-Ray Bursts

Date	Universal Time[a]	GBM Designation[b]	Observed By[c]
2010 Jul 13	23:31:34	GRB100713980	AGI, Kon, MES, MO, RHE, Suz, Swi[d]
2010 Jul 14	16:07:23	GRB100714672	INT
2010 Jul 14	16:27:20	GRB100714686	INT, Kon, Suz
2010 Jul 15	11:27:17	GRB100715477	INT
2010 Jul 17	08:55:06	GRB100717372	AGI, INT, MES, Swi[d]
2010 Jul 17	10:41:47	GRB100717446	INT
2010 Jul 18	03:50:09	GRB100718160	INT, Suz
2010 Jul 18	19:06:22	GRB100718796	Kon
2010 Jul 19	07:28:17	GRB100719311	INT
2010 Jul 19	19:48:08	GRB100719825	INT
2010 Jul 19	23:44:04	GRB100719989	AGI, INT, Kon, MES, Swi[d]
2010 Jul 22	02:18:37	GRB100722096	INT, Kon, MES, Suz, Swi[d]
2010 Jul 22	06:58:24	GRB100722291	INT, Suz
2010 Jul 24	00:42:06	GRB100724029	AGI, INT, Kon, MES, MO, RHE, Suz, Swi[e]
2010 Jul 25	11:24:34	GRB100725475	INT, Kon, RHE, Suz, Swi[e]

Notes.
[a] Universal time is the trigger time of a near-Earth spacecraft.
[b] Four events were listed as UNCERTAIN in the GBM catalog; however, they are likely to be valid cosmic events.
[c] AGI: *Astro-rivelatore Gamma a Immagini LEggero* (*AGILE*); *IKAROS*: *Interplanetary Kite-craft Accelerated by Radiation Of the Sun* INT: *International Gamma-Ray Laboratory*; Kon: *Konus-Wind*; LAT: *Fermi Large Area Telescope*; *MAXI*: *Monitor of All-sky X-ray Image*; MES: *Mercury Surface, Space Environment, Geochemistry, and Ranging* mission; MO: *Mars Odyssey*; RHE: *Ramaty High Energy Solar Spectroscopic Imager*; Suz: *Suzaku*; Swi: *Swift*.
[d] Burst was outside the coded field of view of the BAT, and not localized by it.
[e] Burst was localized by *Swift*-BAT; IPN triangulation cannot improve on this localization.
[f] Burst was localized by *INTEGRAL*-IBIS; IPN triangulation cannot improve on this localization.

(This table is available in its entirety in machine-readable form.)

Table 3
Number of GBM Bursts Observed by Each Spacecraft in Table 2

INTEGRAL	*Konus*	*Swift*	*Suzaku*	*MESSENGER*	*RHESSI*	*Odyssey*	*AGILE*	*IKAROS*	*MAXI*
317	275	195	189	159	89	85	47	17	1

Table 4
Number of Bursts Detected by N IPN Spacecraft in Table 2

$N = 2$	$N = 3$	$N = 4$	$N = 5$	$N = 6$	$N = 7$	$N = 8$	$N = 9$
103	86	65	65	50	42	12	5

Table 5
IPN Annuli for 165 Bursts

GRB Designation	α_1	δ_1	R_1	δR_1	α_2	δ_2	R_2	δR_2
GRB100713980	351.6251	−4.3823	86.7394	0.0691	105.0319	15.7803	27.1131	0.4829
GRB100714672	87.9475	23.6705	73.7966	0.7987	...	...	...	...
GRB100717372	284.069	−16.3674	32.9611	0.414	187.1783	−70.985	86.2573	5.275
GRB100719989	104.1693	16.6924	20.7695	0.4877	94.1428	22.5421	30.9143	1.4075
GRB100722096	284.3243	−17.1181	44.6759	0.3593	...	...	...	...
GRB100724029	104.7297	17.5308	58.8349	0.2804	99.5997	16.2756	61.2102	1.7737
GRB100804104	183.1288	−0.8799	71.6904	0.0489	295.1689	−17.4964	62.5482	1.5403
GRB100805845	114.2386	19.8937	60.8324	0.2447	...	...	...	...
GRB100811108	301.849	−19.9403	58.5094	0.0814	7.0657	2.6719	28.042	0.0932

(This table is available in its entirety in machine-readable form.)

units are degrees, and coordinates are given in epoch J2000, in the heliocentric frame.

The 14 columns in Table 6 give: (1) the designation of the burst, in the *Fermi* format (GRByymmddfff), for the year, month, day, and fraction of the day, (2) the R.A. of the center of the error box, (3) the decl. of the center of the error box, (4) the R.A. of the first error box corner, (5) the decl. of the first error box corner, (6) the R.A. of the second error box corner, (7) the decl. of the second error box corner, (8) the R.A. of the third error box corner, (9) the decl. of the third error box corner,

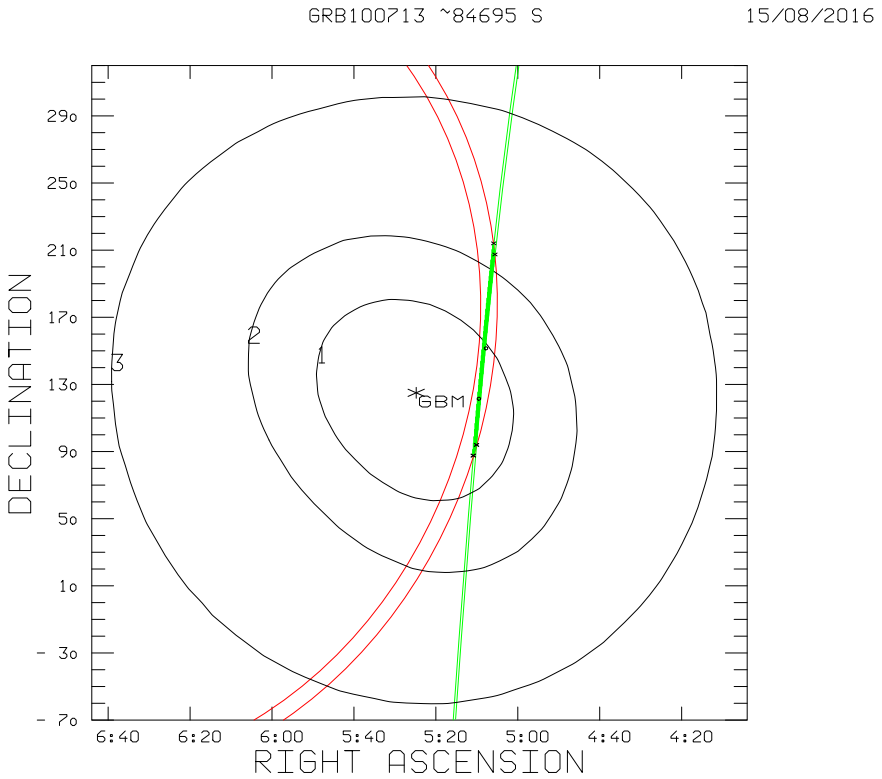

Figure 1. IPN localization of a GBM burst. 1. Date in upper right-hand corner: DD/MM/YYYY when the plot was produced. 2. Date and time above the upper R.A. axis: GRBYYMMDD and the approximate time in seconds of day for the burst. This time is actually a fiducial time used for triangulation, and it may differ from the Earth-crossing time by up to minutes in some cases. 3. R.A., decl.: these are J2000. Not all the figures are to scale; in some cases, changing the aspect ratio displays the IPN error box more clearly. 4. Green lines: annuli obtained by triangulation. These are 3σ statistical plus systematic confidence regions. 5. Green shading: the region that is common to the IPN annulus or annuli. 6. Small circle: the point in the IPN annulus or annuli where the localization probability is a maximum. The coordinates are given in Table 6. The following are present in some figures in the figure set. 1. Red lines: additional triangulation annuli. 2. Turquoise lines: additional triangulation annuli. 3. Small x: the points that define either the IPN/GBM 3σ error box, or the IPN-only 3σ error box. The coordinates are given in Table 6. 4. Black lines labeled ECLIP.: ecliptic latitude band, from *Konus-Wind*. These are generally ∼95% confidence regions. 5. Earth-N: Earth-blocking, as seen from satellite *N*. This region is excluded from the localization. If the satellite is far from Earth, the region may be a point. 6. Mars: Mars-blocking, as seen from Mars *Odyssey*. This region is excluded from the localization. 7. Contours labeled 1, 2, 3: GBM 1σ, 2σ, and 3σ statistical plus systematic confidence contours. 8. Circle labeled GBM: GBM 1σ, statistical-only error circle (where contours are not available). 9. Asterisk labeled GBM: center of the GBM error region. 10. LAT: *Fermi* LAT error circle, statistical only, obtained from GCN Circulars; LAT n: different proposed LAT error circles, from GCN Circulars. 11. Source n: a proposed optical or X-ray counterpart to the GRB, from GCN Circulars. 12. XRT: a proposed Swift XRT counterpart, from GCN Circulars.

(The complete figure set (165 images) is available.)

(10) the R.A. of the fourth error box corner, (11) the decl. of the fourth error box corner, (12) the area of the 3σ GBM error contour, in square degrees, (13) the area of the 3σ IPN error box, in square degrees; if there is a single IPN annulus, this is the area of the entire annulus; if there are two annuli, this is the area of the error box formed by their intersection, (14) the ratio of the GBM area to the IPN area. The coordinate units are degrees, and are given in epoch J2000, in the heliocentric frame. For events with a single IPN annulus, the error box corners are taken to be the intersection of the 3σ annulus with the GBM 3σ contour. For events with two IPN annuli, the error box corners are the points where the annuli intersect. There are 164 entries in the table; the annulus for GRB100814351 (Figure 11 in figure set 1) does not intersect the GBM 3σ contour.

4. A Few Statistics

During the period covered by this catalog, the IPN comprised nine spacecraft. Three of them (*Konus-Wind*, *INTEGRAL*, and *MESSENGER*) were subject to virtually no planet-blocking; all had high duty cycles, with that of *Konus-Wind* in particular exceeding 95%. Thus the probability of any particular GBM burst with flux or fluence above the IPN threshold being observed by at least one other spacecraft in the network was high. Indeed, as Table 4 demonstrates, of the 462 bursts in the second two-year period of the GBM catalog (von Kienlin et al. 2014), 428 (93%) were observed by at least 1 other IPN spacecraft. They are listed in Table 2, and the number of bursts observed by each IPN spacecraft is compiled in Table 3. These events had fluences between 3.3×10^{-8} and 2.2×10^{-4} erg cm^{-2}, peak fluxes between 0.44 and 201 photons cm^{-2} s^{-1}, and durations between 0.05 and 500 s, as measured by the GBM. Figure 2 shows the distributions of peak flux, T90, and fluence of the GBM and IPN bursts. Bursts can be detected by IPN instruments on the basis of their peak flux or their fluence. Thus, it is possible to detect a short-duration event with a high peak flux even though its fluence may be quite small. Those events that were not observed by an IPN spacecraft had fluences between 5.1×10^{-8} and 6.6×10^{-6} erg cm^{-2}, peak fluxes between 0.61 and 4.5 photons cm^{-2} s^{-1}, and durations between 0.32 and 236 s, as measured by the GBM. In the case of the highest fluence missed event, GRB110101506 with fluence 6.6×10^{-6} erg cm^{-2}, the duration was 236 s, leading to a low average flux and a non-detection, even though six other IPN

Table 6
IPN Error Box Coordinates for 164 Bursts

GRB Designation	Center		Corners								GBM Area, sq. deg.	IPN Area, sq. deg.	Ratio, GBM Area/IPN Area
	α_C	δ_C	α_1	δ_1	α_2	δ_2	α_3	δ_3	α_4	δ_4			
bn100713980	77.043	15.062	77.716	8.673	76.470	21.318	77.520	9.309	76.395	20.657	1020	1.660	616.0
bn100714672	331.056	74.826	275.851	83.271	266.642	81.732	349.215	57.801	351.683	58.950	1020	49.800	20.5
bn100717372	318.492	−16.677	318.045	−11.126	318.963	−22.231	317.124	−10.894	318.083	−22.023	13800	9.260	1490.0
bn100719989	114.910	0.855	121.950	4.535	106.315	−4.459	121.947	6.259	109.426	−2.914	581	5.580	104.0
bn100722096	237.825	−14.734	239.208	−10.073	238.256	−10.868	236.926	−18.340	237.579	−19.416	169	11.500	14.7
bn100724029	143.302	71.939	165.398	55.367	68.891	73.066	167.370	45.678	87.382	75.345	652	23.500	27.7
bn100804104	251.605	28.777	251.199	30.675	252.071	26.934	251.105	30.587	251.979	26.842	632	0.374	1690.0

(This table is available in its entirety in machine-readable form.)

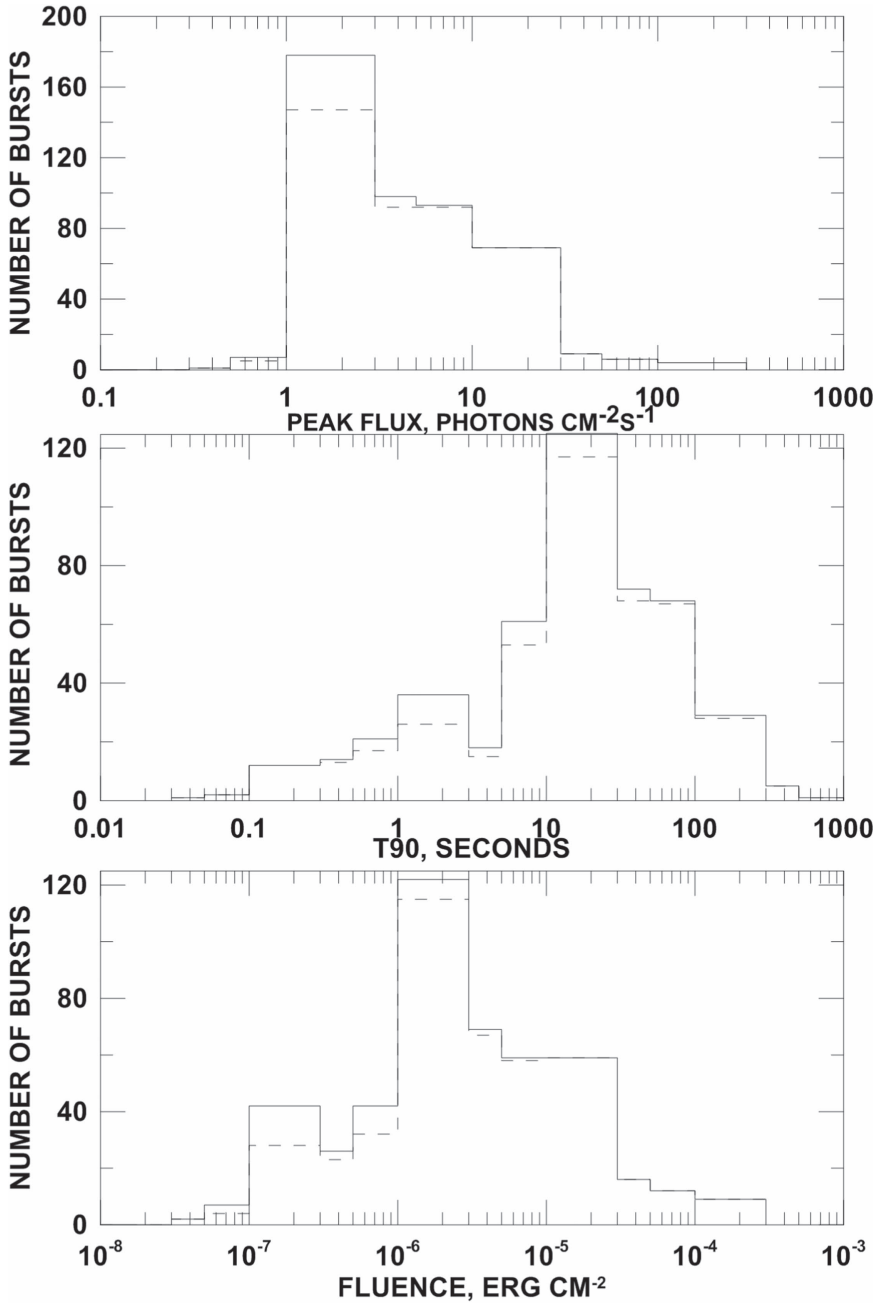

Figure 2. From top to bottom: the distributions of peak flux, T90 duration, and fluence of the bursts in this catalog. The solid lines show the distributions of the 462 GBM bursts, and the dashed lines show the distributions of the 428 IPN bursts detected by at least one other spacecraft.

instruments were operating. For 165 events, it was possible to improve the GBM localizations by triangulation; 85 events were localized to IPN error boxes, and 80 to IPN annuli. The minimum and maximum 3σ IPN annulus half-widths were 3.9×10^{-2} and 15°.8, and the average was 0°.62. The IPN annuli and error boxes have 3σ areas between about 78 square arcminutes and 380 square degrees, and the average area was 27.1 square degrees (median 5.6 square degrees). The GBM fluence, flux, and duration data have been taken from the HEASARC online catalog.[24] The data in Tables 2 and 5 are also available at the IPN website.[25]

There were 82 short-duration events in the second two-year period of the GBM catalog, and 71 of them (87%) were detected by at least one other IPN spacecraft. 22 of the 71 could be localized by triangulation, resulting in an average reduction of the error box size by a factor of over 4300.

To judge the consistency between the IPN and GBM localizations, the following method was used. For the 85 events localized to IPN error boxes, the fraction of the error box within the 1σ, 2σ, and 3σ contours was tabulated, along with the fraction outside the 3σ contours. We found that 47.5, 70.2, and 83.2 events (56%, 83%, and 98%) lay within the 1σ, 2σ, and 3σ contours, and 1.8 (2.1%) lay outside the 3σ contours. If the contours are assumed to follow a two-dimensional circular distribution, the expected numbers are 39%, 86%, 99%, and 1.1%. Thus, the 1σ contours appear to be rather conservatively

[24] http://heasarc.gsfc.nasa.gov/cgi-bin/W3Browse/w3query.pl
[25] http://ssl.berkeley.edu/ipn3/index.html

estimated, while the 2σ and 3σ ones agree closely with the IPN localizations.

5. IPN Events That Are Not in the GBM Catalog

Four events in Table 2 were detected by the GBM and classified as "uncertain," but were observed by other IPN spacecraft. They cannot be localized by triangulation, however. UNCERT10102526 was observed by *INTEGRAL* and *Konus*, which rules out a local origin (TGF or particles) for it. The Konus ecliptic latitude and the GBM localization are coarse, but inconsistent with a solar origin. The most likely origin of this event is cosmic. UNCERT11092348 was observed by *INTEGRAL* and *Suzaku*, again ruling out a local origin. Both the *Fermi* and *Suzaku* localizations are coarse and consistent with the Sun, but the *Suzaku* spectrum is hard and the duration is short, suggesting a cosmic origin. UNCERT11123162 was observed by *Konus* and *INTEGRAL*, ruling out a local origin. *INTEGRAL*'s high lower energy threshold (~80 keV), the lack of obvious solar activity, and the fact that the GBM localization is 57° from the Sun (albeit with a 34° uncertainty) again suggest a cosmic origin. Finally, UNCERT12011729 was observed by *Suzaku*, making a local origin unlikely. The GBM localization is 42° from the Sun, and the uncertainty is 35°. However, the *Suzaku* spectrum is hard and the duration is short, suggesting a cosmic origin. If these four events are indeed cosmic, it would suggest that the GBM catalog is over 99% complete.

6. Conclusion

This catalog is the second installment of the IPN supplements to the GBM burst catalogs. The nine-spacecraft IPN detects a total of about 325 bursts per year (18 of which are short-duration, hard spectrum GRBs; see Pal'shin et al. 2013; Svinkin et al. 2016), has almost no planet-blocking or duty cycle restrictions when all the spacecraft are considered, and is capable of good localization accuracy at the cost of longer delays. There are many ground-based electromagnetic and non-electromagnetic experiments that can take advantage of either IPN error boxes for events not observed by the GBM, or of the IPN improvements to GBM contours, and for which delays are not an issue. For example, the IPN search for a counterpart to GW150914 was described in Hurley et al. (2016), and a search for gravitational radiation associated with short-duration IPN bursts is underway. The IPN can also respond to Astrophysical Multimessenger Observatory Network (AMON) alerts.

Support for the IPN was provided by NASA grants NNX09AU03G, NNX10AU34G, and NNX11AP96G (*Fermi*), NNX09AR28G and NNX08AX95G (*INTEGRAL*), NNX10AI23G and NNX12AD68G (*Swift*), NNX09AV61G and NNX10AR12G (*Suzaku*), NNX07AR71G (*MESSENGER*), and JPL Contracts 1282043 and Y503559 (*Odyssey*). The *Konus-Wind* experiment is supported by a Russian Space Agency contract and RFBR grant 12-02-00032-a. R.L.A. and S.V.G. gratefully acknowledge support from RFBR grants 15-02-00532-i and 16-29-13009-ofi-m. This research has made use of data and/or software provided by the High Energy Astrophysics Science Archive Research Center (HEASARC), which is a service of the Astrophysics Science Division at NASA/GSFC and the High Energy Astrophysics Division of the Smithsonian Astrophysical Observatory.

References

Aptekar, R., Frederiks, D., Golenetskii, S., et al. 1995, SSRv, 71, 265
Atwood, W., Abdo, A., Ackermann, M., et al. 2009, ApJ, 697, 1071
Connaughton, V., Briggs, M., Goldstein, A., et al. 2015, ApJS, 216, 32
Del Monte, E., Feroci, M., Pacciani, L., et al. 2008, A&A, 478, L5
Gehrels, N., Chincarini, G., Giommi, P., et al. 2004, ApJ, 611, 1005
Gold, R., Solomon, S., McNutt, R., et al. 2001, P&SS, 49, 1467
Hurley, K., Atteia, J.-L., Barraud, C., et al. 2011, ApJS, 197, 34
Hurley, K., Briggs, M., Kippen, R. M., et al. 1999a, ApJS, 120, 399
Hurley, K., Briggs, M., Kippen, R. M., et al. 1999b, ApJS, 122, 497
Hurley, K., Briggs, M., Kippen, R. M., et al. 2011, ApJS, 196, 1
Hurley, K., Guidorzi, C., Frontera, F., et al. 2010, ApJS, 191, 179
Hurley, K., Kouveliotou, C., Cline, T., et al. 2000a, ApJ, 537, 953
Hurley, K., Laros, J., Brandt, S., et al. 2000b, ApJ, 533, 884
Hurley, K., Lund, N., Brandt, S., et al. 2000c, ApJS, 128, 549
Hurley, K., Mitrofanov, I., Kozyrev, A., et al. 2006, ApJS, 164, 124
Hurley, K., Pal'shin, V., Aptekar, R., et al. 2013, ApJS, 207, 39
Hurley, K., Stern, B., Kommers, J., et al. 2005, ApJS, 156, 217
Hurley, K., Svinkin, D., Aptekar, R., et al. 2016, ApJL, 829, L12
Laros, J., Boynton, W., Hurley, K., et al. 1997, ApJS, 110, 157
Laros, J., Hurley, K., Fenimore, E., et al. 1998, ApJS, 118, 391
Marisaldi, M., Labanti, C., Fuschino, F., et al. 2008, A&A, 490, 1151
Meegan, C., Lichti, G., Bhat, P. N., et al. 2009, ApJ, 702, 791
Paciesas, W., Meegan, C., von Kienlin, A., et al. 2012, ApJS, 199, 18
Pal'shin, V., Hurley, K., Svinkin, D., et al. 2013, ApJS, 207, 38
Rau, A., von Kienlin, A., Hurley, K., & Lichti, G. 2005, A&A, 438, 1175
Serino, M., Sakamoto, T., Kawai, N., et al. 2014, PASJ, 66, 87
Smith, D. M., Lin, R., Turin, P., et al. 2002, SoPh, 210, 33
Svinkin, D., Frederiks, D., Aptekar, R., et al. 2016, ApJS, 224, 10
Takahashi, T., Abe, K., Endo, M., et al. 2007, PASJ, 59, 35
Tavani, M., Barbiellini, G., Argan, A., et al. 2009, A&A, 502, 995
von Kienlin, A., Meegan, C., Paciesas, W., et al. 2014, ApJS, 211, 13
Yamaoka, K., Endo, A., Enoto, T., et al. 2009, PASJ, 61, S35
Yonetoku, D., Murakami, T., Gunji, S., et al. 2011, PASJ, 63, 625